ORIGINAL PAPER

DOI: http://dx.doi.org/10.15403/jgld-4997

Color Mapping using Ultrasound System-integrated Perfusion Software for Evaluation of Focal Liver Lesions: A Possible First Step for More Independent Reading

Ivor Dropco[1*], Ulrich Kaiser[2*], Lola Wagner[3], Stefan M Brunner[1], Hans Jürgen Schlitt[1], Christian Stroszcynski[3], Friedrich Jung[4], Dong Yi[5], Wolfgang Herr[2], Ernst Michael Jung[3]

1) Clinic and Polyclinic for Surgery, University Hospital Regensburg, Regensburg, Germany;
2) Medical Clinic and Polyclinic III, University Hospital Regensburg, Regensburg, Germany
3) Institute for Diagnostic Radiology and Interdisciplinary Ultrasound, University Hospital Regensburg, Regensburg, Germany
4) Institute of Biotechnology, Molecular Cell Biology, Brandenburg University of Technology, Senftenberg, Germany
5) Department of Ultrasound Zhongshan Hospital, Fudan University, Shanghai, China

Address for correspondence:
Ivor Dropco
Clinic and Polyclinic for Surgery, University Hospital Regensburg, Regensburg, Germany
ivor.dropco@ukr.de;

Received: 01.05.2023
Accepted: 17.08.2023

*equal contribution

ABSTRACT

Aims: To assess the value of using integrated parametric ultrasound software for contrast-enhanced ultrasonography (CEUS) of liver tumors.
Methods: 107 patients with liver tumors were studied. CEUS were performed to detect focal lesions. Parametric images were based on continuous CINE LOOPs, from the early-arterial phase (15 s) to the portal-venous phase (1 min) generated by perfusion software. The evaluations of the parametric images and their dignity for liver lesions were performed independently by an experienced and a less-experienced investigator. Computed tomography, magnetic resonance imaging scans or histological analysis were used as references.
Results: High parametric image quality were obtained in all patients. Among the patients, 44% lesions were benign, 56% were malignant. The experienced investigator correctly classified 46 of 47 (98%) as benign, and 60 of 60 (100%) as malignant tumors based on the parametric images. The less-experienced investigator correctly classified 39 of 47 (83%) as benign, and 49 of 60 (82%) malignant tumors, acheaving a high statistical accuracy of 98% with this type of diagnostic.
Conclusion: Parametric imaging for grading the malignant degree of tumor may be a good complement to existing ultrasound techniques and was particularly helpful for improving the assessments of the less-experienced examiner.

Key words: CEUS – parametric imaging – dynamic vascularization – liver malignancies.

Abbreviations: CCC: cholangiocellular carcinoma; CEUS: contrast-enhanced ultrasonography; CHI: contrast harmonic imaging; CINE-LOOP: digital movie storage of real-time images in chronological order, with the possibility of subsequent playback; CT: computed tomography; DEGUM: German Society for Ultrasound in Medicine; DICOM: digital imaging and communications in medicine; FNH: focal nodular hyperplasia; FSUMB: European Federation of Societies for Ultrasound in Medicine and Biology; HCC: hepatocellular carcinoma; HIFI: high-intensity focused; MRI: magnetic resonance imaging; MWA: microwave ablation; PACS: Picture Archiving and Communication System; RFA: radiofrequency ablation; TACE: transarterial chemoembolization.

INTRODUCTION

Despite ongoing progress in the identification of benign and malignant liver lesions with the aid of contrast-enhanced ultrasonography (CEUS), the significance of the results crucially depends on the experience of the examiner, examination conditions, and image quality [1], which limits the clinical applications and interpretation. The high diagnostic significance of CEUS for characterization of liver tumors has previously been demonstrated in numerous studies, including multicenter studies of the German Society for Ultrasound in Medicine (DEGUM) [2-5]. Depending on the tumor size and tumor entity, a high diagnostic certainty > 90% can be achieved [6]. Tumors have standard characterizations in wash-in and wash-out sequences using dynamic evaluation of contrast agent kinetics in tissue. However, a variety of limitations, such as limited experience of the examining person, inhomogeneous liver tissue, deep-seated lesions, or overlays (e.g., by other organs), may lead to limitations in diagnostic confidence in daily routines [7-9]. A color-based image evaluation using artificially-generated parametric color-coded images can be a solution to this problem and provide a more objective

assessment of degree of malignancy [10-12]. Based on CEUS kinetics, this method can be used to generate, store, and evaluate data in a dynamic digital imaging and communications in medicine (DICOM) digital movie storage of real-time images in chronological order, with the possibility of subsequent playback (CINE-LOOP) format. In addition, color-based image evaluation is made possible by means of the software integrated in the ultrasound device used. This evaluation can subsequently provide good diagnostic confidence even for inexperienced examiners [13]. This study aimed to evaluate the extent to which parametric false-color imaging of CEUS in liver lesions can contribute to improved diagnostics.

METHODS

Ethics

The University of Regensburg approved this study and the retrospective analysis of CEUS and its perfusion images (Ethics No. 20-2122-104).

Patients' Collective

A total of 107 patients, 64 males (59.8%, median age of 66 with standard deviation of ± 15) and 43 females (40.2%, median age of 54 with standard deviation of ± 18), were retrospectively studied by CEUS over a 4-year period (Table I). A prerequisite for patient recruitment was contrast-enhanced magnetic resonance imaging (MRI) or computed tomography (CT) or, in individual cases, histopathological examination of the existing lesions of the liver to enable comparative diagnosis. The CEUS examination was performed by an experienced examiner (>3000 examinations per year for 20 years) using a high-resolution multifrequency convex transducer (1–6 MHz). The procedure chosen in the present study was CEUS, which was subsequently evaluated using the device-integrated perfusion software. Written informed consent was obtained from the patients for all examinations. A contrast agent allergy was considered a contraindication.

Table I. Basic demographic characteristics of the enrolled patients

	N (%)	Age/Median [SD (±)]
	107 (100)	61 (± 15)
Gender		
Male	64 (59.8)	66 (± 12)
Female	43 (40.2)	54 (± 18)

Data are presented as means with standard deviations (SDs) for women, men, and all patients.

Examination Technique

The examinations were performed according to the European Federation of Societies for Ultrasound in Medicine and Biology (EFSUMB) guidelines and based on the multicenter DEGUM study [3]. Lesions were first examined by B-scan ultrasound using a high-end device (LOGIQ E9, GE, Milwaukee, WI, USA) and a convex transducer (1–6 MHz). Macrovascularization was then assessed by power Doppler and color-coded Doppler sonography. For the subsequent examination with CEUS, 1.0–2.4 mL i.v. contrast medium (SonoVue®, Bracco, Milan, Italy) was used followed by a bolus administration of 5–10 mL of 0.9% saline solution. SonoVue® is a second-generation contrast agent. The sulfur hexafluoride microbubbles have a phospholipid coating that accumulates in the blood. The microbubbles have a diameter of 2–10 µm, are strictly intravascular, and can pass through the capillaries. The interface between sulfur hexafluoride gas and blood reflects the ultrasound waves, enhancing the contrast between the tissue and blood. Finally, digital DICOM loops of 1 min from the onset to the beginning of the arterial outflow of the contrast medium (and then short follow-up sequences up to the late phase of 5–6 min) were stored in the Picture Archiving and Communication System (PACS).

Characterization of Liver Lesions by CEUS

The typical characteristics of benign liver lesions are progressive enhancement without late wash-out, nodular from the margin in hemangiomas, radicular in focal nodular hyperplasia (FNH), and from the margin to the center in adenomas. Malignant lesions typically show irregular arterial contrast in metastases starting from the margin (especially colorectal tumor sites) and in hepatocellular carcinoma (HCC) and cholangiocellular carcinoma (CCC) in the center with subsequent increasing wash-out towards the late phase. In the low-mechanical index (MI) technique, the enhancement patterns correspond to those known from contrast-enhanced CT [14]. After chemotherapy or ablative procedures, such as radiofrequency ablation (RFA), microwave ablation (MWA), irreversible electroporation, or even after transarterial chemoembolization (TACE), the goal was to devascularize the formerly irregularly hypervascularized tumor areas as completely as possible. Residual tumors were characterized by irregular hypervascularization in the early arterial phase and wash-out in the late phase (Table II).

Table II. Underlying disease and size of lesions in all patients

	n	%	Size in mm Median (range)
FNH	11	10.3	50 (25–100)
Cystic lesion	5	4.7	16 (15–40)
Hemangioma	8	7.5	39 (14–60)
Adenoma	1	0.1	25 (1)
Resection without reccurence	7	6.5	25 (15–40)
MWA	12	11.2	45 (23–60)
MWA and resection	2	1.9	43.5 (37–50)
IRE	1	0.1	23 (1)
Metastasis	14	13.1	26 (10–90)
CCC	5	4.7	50 (28–60)
HCC/CCC	1	0.1	33 (1)
HCC	23	21.5	40 (13–160)
Hemangioendothelioma	1	0.1	120 (1)
TACE with recurrence	2	1.9	20 (15–45))
MWA with recurrence	6	5.6	12 (10–15)
Resection with recurrence	5	4.7	18 (12–50)
Metastasis with a cyst	2	1.9	20 (10–30)
HCC with a dysplastic node	1	0.1	18 (1)

FNH: focal nodular hyperplasia; MWA: microwave ablation; IRE: irreversible electroporation; CCC: cholangiocellular carcinoma; HCC: hepatocellular carcinoma; HCC/CCC: mixed types; TACE: transarterial chemoembolization.

Examination by CT, MRI, and Histology

Computed tomography was performed as at least two-phase CT with arterial and portal venous phases, and with late phase (after 3 min) if HCC or CCC was suspected. A multislice CT, dual source (Somatom Definition Flash®, Siemens, Erlangen, Germany) with bolus triggering of 80–110 mL of contrast medium i.v. (Accupaque™ 350 mg, GE Helthcare Buchler GmbH & Co. KG) was used after obtaining written consent and consideration of possible contraindications. The reconstruction interval was 5-mm axially and coronally. Magnetic resonance imaging was performed on a 3 Tesla instrument (Skyra®, Siemen, Erlangen Germany) native with T2- and T1-weighting, diffusion with apparent diffusion coefficient (ADC Maps) and dynamic contrast imaging with 3D Vibe sequences and the Reticulo-Endothelial System (RES) specific contrast agent (Primovist®, Bayer Vital GmbH, Germany) after written consent and consideration of contraindications. The biopsies were performed under ultrasound or CT control or based on histology taken intraoperatively.

Parametric Imaging

As a prerequisite for obtaining parametric images from the preliminary CEUS examinations, the images were required to be digitally recorded without relevant motion artifacts and with well-defined lesions. The stored DICOM loops were processed by an experienced examiner. Parametric images were generated using device-integrated perfusion software. In this respect, the parametric analysis more clearly highlights the dynamics of microbubbles in corresponding false colors in the time interval. Thus, after contrast agent administration, the device-integrated software can already create an autonomous image sequence with color-coded images in the early arterial phase. The software algorithm for interpreting dynamic vascularization does not require any manual adjustments by the examiner and can therefore generate reproducible results. In this regard, a parametric evaluation allows objective, machine-assisted image evaluation and analysis with respect to changes in microvascularization or in the wash-in phase. The false colors were chosen as follows: red for extensive hypervascularization, orange for marked hypervascularization, yellow for partial hypervascularization, green for proportional vascularization, and blue to purple only for minor vascularization. Whether or not vascularization was parametrically with CEUS on dynamic centrifugal or centripetal microvascularization, respectively, regular or irregular, was assessed.

Ultrasound Image Analysis

The combined interpretation of ultrasound images in B-scan ultrasound and CEUS was assessed by an experienced examiner. The parametrically generated images were separately evaluated independently by an experienced and a less-experienced examiner without relevant previous knowledge in ultrasound diagnostics. The perfusion pattern of the false colors was used to determine if the liver lesion was benign or malignant (Table III).

Verification of the Final Diagnosis

Verification of the diagnoses was performed by matching using additional imaging modalities, such as contrast-enhanced CT or MRI or by an existing histopathologic examination. Thus, only patients whose lesions were most likely confirmed were finally evaluated.

Statistical Analysis

All results were described as the arithmetic mean and standard deviation. To calculate the sensitivity, specificity, positive predictive value, and negative predictive value of ultrasound for confirmation, the following formulas were used based on the agreed 2×2 table: Sensitivity=TP/(TP+FN), Specificity=TN/(FP+TN), Positive predictive value=TP/(TP+FP), Negative predictive value=TN/(FN+TN), and Accuracy=(TP+TN)/(TP+TN+FP+FN) where TP stands for diagnosis recognized as correct, TN stands for unclear diagnosis, TP and TN are the sum for all malignant and benign tumors, and FN stands for benign (FP) and malignant (FN) descriptions assessed by parametric ultrasound. Each cross-tabulation was calculated separately once for the experienced investigator and once for the less-experienced investigator (Table IV).

RESULTS

A total of 107 patients were examined in this study. Of these, 43 were females and 64 were males. Their mean age was 62 years, and the youngest person was 19 and the oldest was 85 years (Table I). Corresponding CT, MRI, or histology of the relevant anatomy was available for all patients. The basis for the creation of parametric images is CEUS, whereby the dignity of the liver lesions was additionally verified. Correlating to histology, MRI, or CT, depending on tumor type, all benign (n=47, 100%) and all malignant (n=60, 100%) tumors were identified as correct (Table III). Magnetic resonance imaging

Table III. Analysis of patients with clinical suspicion of liver disease by CEUS, CEUS with parametric imaging, CT or MRI or histopathology considering malignancy grade

Malignancy suspicion in CT/MRI/Histology	US + CEUS Liver Suspicion n (%)	Parametric Imaging Examiner 1 Liver Suspicion n (%)	Parametric Imaging Examiner 2 Liver Suspicion n (%)
Benign Lesion n = 47	Yes 47 (100)	Yes 46 (98)	Yes 39 (83)
	No 0 (0)	No 1 (2)	No 8 (17)
Malignant Lesion n = 60	Yes 60 (100)	Yes 60 (100)	Yes 49 (82)
	No 0 (0)	No 0 (0)	No 11 (18)

Listed below "No" for images that are not assessable due to insufficient image quality. US: ultrasound; CEUS: contrast-enhanced ultrasound; Examiner 1: experienced examiner; Examiner 2: less-experienced examiner; CT: computed tomography; MRI: magnetic resonance imaging.

Table IV. Diagnostic accuracy, sensitivity, and specificity for every examination technique

	Specificity	Sensitivity	PPV	NPV	Accuracy
Examiner 1	100%	100%	100%	100%	100%
Examiner 2	95%	100%	96%	100%	98%

Diagnostic accuracy for all benign and malignant liver lessions for an experienced and less-experienced examiner. Examiner 1: experienced examiner; Examiner 2: less-experienced examiner. PPV: positive predictive value; NPV: negative predictive value.

was performed in 35 of 47 patients (74%), and CT was performed in 15 of 47 patients (32%) with benign lesions. Two patients with benign lesions (4%) were histologically examined and confirmed, although no MRI or CT scan was performed. Furthermore, 32 of 60 patients (53%) with malignant lesions underwent MRI examination to assess the lesions' dignity, and 39 of 60 patients (65%) underwent a CT examination. In 3 of 60 (5%) patients with malignant disease, no corresponding images were performed, but histological examination is also available here. Overall, histological analysis in the malignant area was performed in 23 patients (38%). Tumor size was documented in all 107 patients (36 from 10 to <30 mm, 45 from 30 to <50 mm, and 26 >50 mm with respect to the largest lesion per patient) (Table III).

Among benign lesions, 11 (10.3%) FNH lesions, 5 (4.7%) cystic lesions, 8 (7.5%) hemangiomas, 1 (0.1%) adenoma, 12 (11.2%) MWA wounds, and 2 (1.9%) MWAs with resection were studied. For example, in an FNH with a typical regular vascularization pattern from the center to the edge, a clearly demarcated hypervascularized lesion with a wheel-storage pattern in red and the central scar in green/blue can be seen with the aid of false colors in Figure 1. To examine correlations with the FNH, an MRI examination (gold standard) was performed and showed a typical smooth-bounding structure in the early arterial contrast media enhancement. Hemangiomas typically show a peripheral nodular enhancement from the edge that continuously increases, whereas adenomas show increasing enhancement from the margin, without late wash-out. Cystic lesions should be avascular.

Among malignant lesions, 23 (21.5%) HCCs, 14 (13.1%) metastases, and 5 (4.7%) CCCs comprised the largest groups. A total of 13 (12%) hepatic recurrences after either resection, MWA or TACE, was studied. The size of the lesions varied from 5 to 160 mm. Images of HCC are characterized by marked irregular hypervascularization during the arterial phase in CEUS and in false-color analysis. As shown in Fig. 2, the internal vascularization is clearly visible with central red color and peripheral yellow. Unlike HCC, CCC in the arterial phase is centrally hypoenhanced in CEUS images; after performing parametric imaging, hypervascularization can be seen in red in the peripheral region (Fig. 3). Metastases with early enhancement in the arterial phase relative to the surrounding tissue are especially noticeable in the CEUS image. False-color analysis shows a clearer distinct hypervascularization (red) (Fig. 4). An avascular area, representing the smallest group of characteristic findings after ablation procedures, can be seen on CEUS; however, with the aid of parametric image coding, recurrence can be more clearly highlighted in the marginal areas of the ablation sites (Fig. 5).

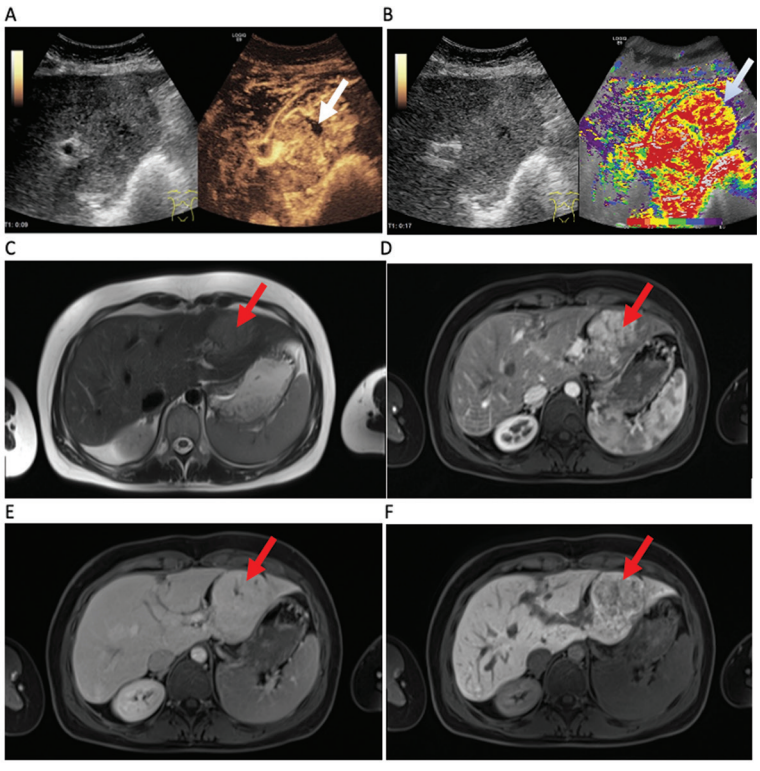

Fig. 1. The case of a 28-year-old female patient with focal nodular hyperplasia (FNH) and a diameter of 6.9 cm in the left liver lobe (Seg II/III).
A: B-scan US: The FNH is difficult to delineate, the lesion is isointense, and the central scar is hypointense. Contrast-enhanced ultrasound (CEUS) 9 s after contrast medium injection. A clearly demarcated lesion is seen with a central scar, feeding vessel, and a classic wheel-spoke pattern (white arrow). B: FNH in B-scan US and CEUS with false-color analysis: Shown is the clearly demarcated hypervascularized lesion (gray arrow), feeding vessel, and wheel-spoke pattern in red, and the central scar in green/blue as a sign of reduced perfusion. C: T2-weighted magnetic resonance imaging (MRI) native image: Visualization of a 6.9-cm (FNH) (red arrow) in the left lobe of the liver (Seg II/III) as a mildly hyperintense lesion. D: Inclusion shown in the T1-weighted MRI: the FNH shows significant contrast enhancement in the early arterial phase after contrast administration of 7 mL of Primovist. E: During the portal venous phase, the contrast of the lesion is aligned with that of the surrounding liver tissue. The central scar without contrast enhancement is clearly visible. F: In the late phase, there is a slight wash-out of the clearly demarcated FNH, especially centrally, whereas the contrast medium is still clearly enriched in the periphery.

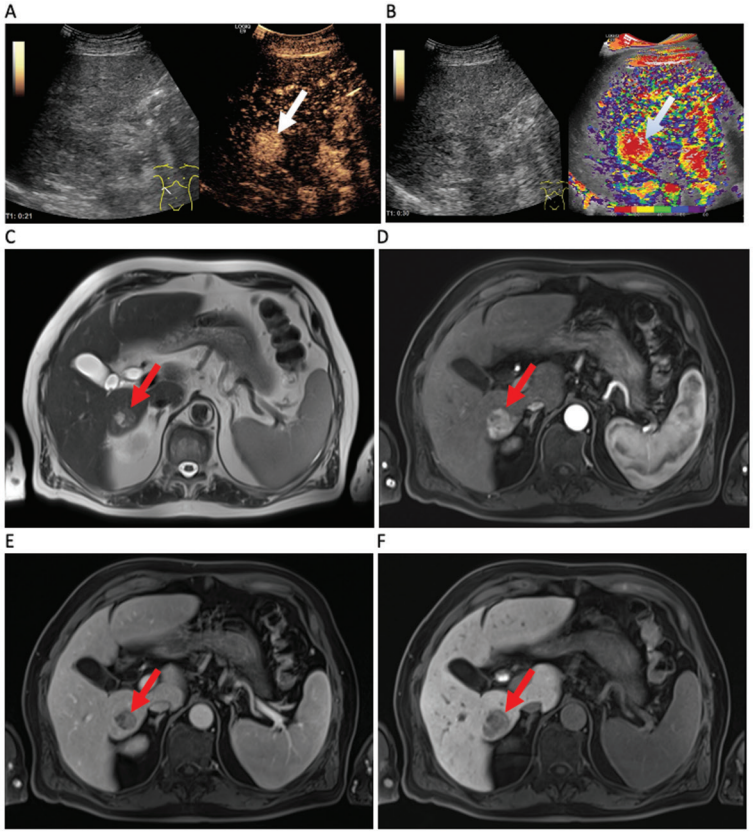

Fig. 2. The case of an 81-year-old patient with two foci of hepatocellular carcinoma (HCC) in segments VI and VIII (diameters: 30 mm and 8 mm).
A: B-scan US and contrast-enhanced ultrasound (CEUS) 21 s after contrast injection. The HCC focus is characterized by marked hypervascularization during the arterial phase (white arrow). B: HCC on B-scan US and contrast-enhanced ultrasound with false-color analysis. Marked hypervascularization during wash-in and typical internal vascularization in HCC (central red, peripheral yellow, marked with gray arrow) of the large foci are clearly visible. C: Native image in T2-weighted magnetic resonance imaging: Visualization of a 3.6-cm hepatocellular carcinoma lesion in the center of segment VI as a hyperintense lesion (red arrow). D: T1-weighted magnetic resonance imaging: After contrast administration of 8 mL of Primovist, a clearly hypercontrast lesion is seen in the early arterial phase. E: The lesion shows a clear wash-out in the portal venous phase and is already hypointense on presentation. F: The late phase also shows a hypointense lesion with clear wash-out.

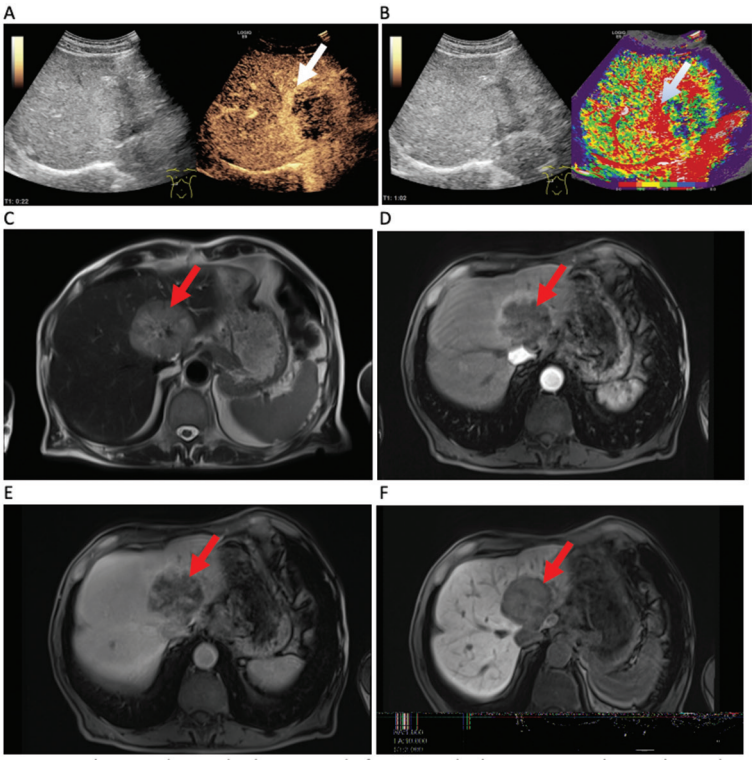

Fig. 3. A 79-year-old patient with a 5 × 6-cm diameter cholangiocellular carcinoma (CCC) centrally located in segments VI, V, and I.
A: B-scan ultrasound: mixed echogenic radiofrequncy. The lesion appears hypoenhanced centrally in the arterial phase, whereas in the periphery there is more contrast enhancement (white arrow), typical of large CCCs. B: The reduced contrast agent accumulation in the center is also indicated in the false-color analysis by the coloration predominantly in blue and green. The lesion appears blurred, and the border area is predominantly red showing hypervascularization (gray arrow). C: Native image in T2-weighted magnetic resonance imaging: Central region of the liver in segment IVa, but also extending into segments I, II, and VIII; the tumor appears as a hyperintense mass measuring approximately 6.3 cm (red arrow). D: In the early arterial phase, contrast enhancement typical of cholangiocellular carcinoma CCC is seen in the marginal area of the lesion. E: During the portal venous phase, there is already a partial wash-out of the lesion (finding: contrast increasing in a flat manner). F: In the hepatobiliary late phase, the tumor is visualized without contrast enhancement.

After correlation with cross-sectional imaging (MRI, CT) and histological analysis, parametric images evaluated by an experienced investigator correctly identified 46 of 47 (98%) as benign lesions. One (2%) lesion was not evaluated because it showed no contrast pattern in the condition after MWA without recurrence. For comparison, benign lesions were also correctly identified in 39 (83%) patients by an inexperienced examiner but could not be described in the remaining 8 (17%) patients. Among the malignant lesions, all 60 were identified based on the color-coded images as malignant by the experienced investigator. The less-experienced examiner correctly identified 49 (82%) lesions as malignant, but the

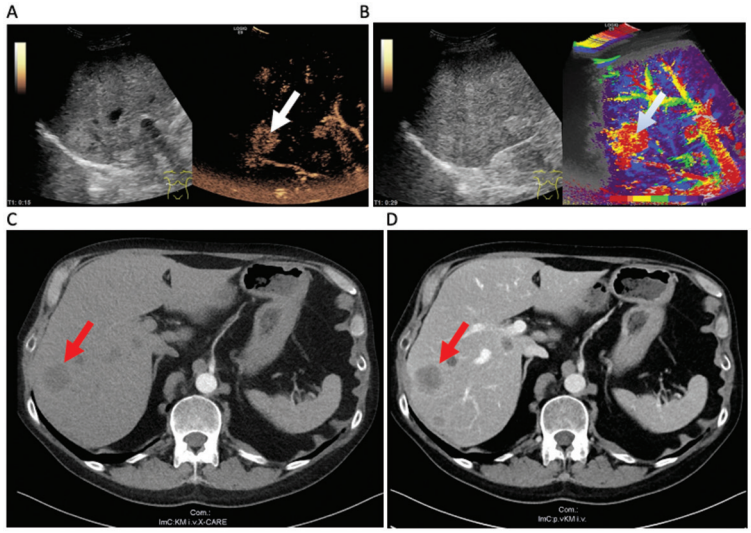

Fig. 4. Case of a 46-year-old patient with multiple hepatic metastases from small-cell lung cancer.
A: B-scan ultrasound: Slightly hyperechogenic metastases that are difficult to delineate. Contrast-enhanced ultrasound: 15 s after contrast medium injection, accumulation in the arterial vessels and metastases is shown (white arrow), but no contrast medium is yet present in the surrounding tissue. B: CEUS parametric: Clearly identifiable vascular structures (red/hypervascularized) with multiple hypervascularized metastases (gray arrows). In the largest lesion, more severe hypervascularization is observed peripherally (peripheral red, central yellow). Computed tomography: Diffusely distributed metastases in both lobes of the liver. C: Native image: in the axial section, the metastases are recognizable as hypodense lesions. D: After contrast agent administration: the metastases are visible in the axial section as lesions without contrast medium accumulation (red arrow).

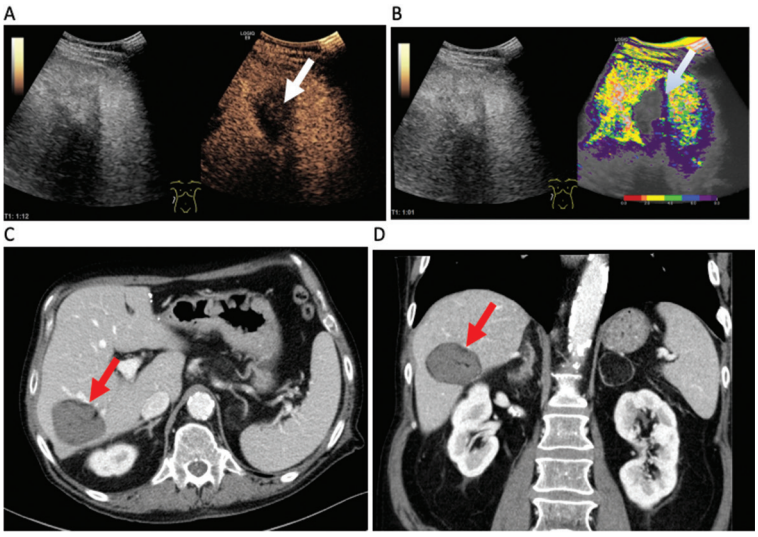

Fig. 5. The case of a 60-year-old patient with an ablation defect (5.5 cm in diameter) after microwave ablation for a rectal metastasis from colorectal carcinoma.
A: In contrast-enhanced ultrasound, the ablation defect can be seen through the recess of contrast material (white arrow) surrounded by uniformly contrasted liver tissue. B: CEUS parametric: clearly devascularized defect centrally (colorless, gray arrow) without hypervascularities at the periphery, indicating tumor recurrence. Computed tomography with contrast agent: 5.5-cm ablation defect in segment VII appears hypodense in both axial (C) and coronal (red arrow) (D) cross-sectional images due to lack of contrast enhancement

remaining 11 could not be assessed (Table III), which gave an accuracy of 98% (Table IV) for this type of diagnostic. Overall, the inexperienced investigator failed to correctly assess 19 of 107 (18%) lesions, whereas the experienced investigator failed to correctly identify only one (2%) lesion.

DISCUSSION

The study results demonstrated that high diagnostic confidence was obtained for CEUS supplemented with parametric false-color evaluation of liver tumors and their perfusion changes. A reliable distinction can be made between benign and malignant lesions, and the microvascularization of liver lesions can be differentiated from changes of non-tumoral origin [2, 3, 12]. Typical of benign lesions is rapid regular contrast enhancement, such as nodular from the edge in hemangiomas, radiolucent from the center in FNH, from edge to center in adenomas, and homogeneous areal enhancement in localized reduced lipids [5]. Malignant lesions show irregular vascularization as early contrast inhomogeneity from the margin in metastases, inhomogeneity irregular from the center in HCC and CCC lesions or rare tumors, such as neuroendocrine tumors [15]. Microshunts exhibit rapid contrast transfer, locally segmental from arterial microvessels into the portal venous system from 15–45 s during the arterial phase. However, inferior perfusion is recognizable as segmentally-delayed contrast enhancement [16].

Contrast-enhanced ultrasound of the liver has high diagnostic value when evaluated by experienced investigators [13]. In the DEGUM multicenter studies, under appropriate examination conditions, CEUS has been shown to have diagnostic reliability comparable to that of contrast-enhanced CT for detection and characterization of solid liver lesions [17, 18]. Compared with contrast-enhanced MRI [19], there may be diagnostic advantages of MRI over CEUS with respect to the detection and characterization of solid liver lesions because of the use of liver-specific MRI contrast agents [20-22].

Nevertheless, randomized studies with large patient cohorts showed diagnostic certainty for both benign and malignant liver lesions, producing a reliable examination result using CEUS [23].

Second-generation ultrasound contrast agents are based on the principle of echo signal amplification by oscillating microbubbles using contrast harmonic imaging (CHI) with a low mechanical index of <0.2. A variety of applications have been described that related to liver diagnostics and non-liver

indications in the EFSUMB guidelines [3]. These guidelines classify the diagnostic relevance of CEUS for liver tumors as high, as done by the FDA, among other agencies, with recommendations for applications regarding pediatric issues [7, 24].

The potential side effects of CEUS are considered to be low, which has led to increasing clinical use worldwide. There is no restriction because of renal function considerations and no influence of ultrasound contrast agents on thyroid metabolism, so CEUS can be used for examination of the liver even in patients with impaired renal function for whom CT or MRI contrast agents are no longer possible [25]. The most common ultrasound contrast agent currently used in Europe is based on sulphur hexafluoride microbubbles (SonoVue®, BRACCO, Italy), which is usually administered intravenously as a bolus (1 to 2.4 mL) followed by 5 to 10 mL of NaCl. Liver-specific ultrasound contrast agents are being researched but are currently not approved for routine use in liver ultrasound diagnostics in Germany and many European countries [26]. To further optimize CEUS with respect to image quality when applying sulphur hexafluoride microbubbles, a number of technical developments have been made. There is increasing use of high-resolution multifrequency transducers with significantly increased crystal counts, modified CHI programs with improved amplitude modulation or pulse inversion techniques, and improved digital image storage, especially of CINE sequences [10, 27]. Furthermore, an attempt has been made to increase the frame rate to achieve a higher level of detail. One possible novel contrast medium ultrasound technique that attempts to take advantage of all of the latest technical developments is high-intensity focused (HIFI) CEUS [28].

Whether or not there are diagnostic advantages for CEUS with a novel mode of investigation, such as HIFI, must be decided after further studies regarding diagnostic safety, detection, and characterization of solid liver tumors; differentiation of complicated cystic lesions; and dynamic acquisition and digital storage of the dynamics of unclear lesions on CT or MRI from the early arterial phase after 10–15 s to a late phase of 5–6 min [29, 30]. Furthermore, CEUS brings an advantage in certain cases of patient with liver cirrhosis, as it provides a non-invasive method for generic cirrhosis of the liver using parametric images (CEUS-PAT) [31].

Image quality is critical for parametric characterization, which can only be sufficiently useful if the images are free of low-intensity artifacts. In particular, the neovascularities in the marginal area are parametrically visualized very well with the use of false colors [12, 32, 33]. For final characterization, however, the original images must always be taken into account until the late wash-out phase after 5–6 minutes. Accordingly, the false-color representation facilitates visualization and characterization for less-experienced examiners [34]. This study provides the first approach for evaluation using artificial intelligence, which can be used to better represent the visualization and dynamics of arterial neovascularization of liver lesions [35-37].

However, there were some study limitations of a technical and clinical nature that should be considered. High-quality examinations require that images of the lesions for characterization be displayed without relevant artifacts over the arterial phase in CEUS and as stored DICOM loops to enable parametric evaluation of them with false colors [13]. Primarily, the evaluation is focused on one target lesion. The evaluation with the false colors takes a maximum of 10 seconds. In the case of multiple lesions, FLASH kinetics would have to be used after the late phase or another contrast agent application would have to be performed. However, this does not apply to routine protocols. The software is also device dependent. Contrast-enhanced ultrasound dynamics and dynamic microvascularization are also influenced by transducer technology, the surrounding tissue, depth localization, and possible superposition [38].

CONCLUSIONS

Contrast-enhanced ultrasound with color-coded image evaluations for primary and secondary liver tumors is technically feasible in principle, even for less-experienced investigators, and can potentially serve as a valid diagnostic tool for rapid, reliable, and more autonomous delineation of malignant and benign liver tumors but is subject to the limitations outlined above. The high diagnostic confidence of CEUS with parametric imaging of the arterial phase of liver lesions and perfusion changes in false colors still pose challenges in the future because of the need to ensure diagnostic validity in clinical practice. Results for the evaluations of artificial intelligence could facilitate the confirmation of diagnostic certainty, but such results should be obtained in a multicenter study.

Conflicts of interest: None to declare.

Authors' contributions: I.D., U.K. and E.M.J. conceived the study. I.D. and U.K. drafted the manuscript. E.M.J., H.J.S., C.S, F.J., D.Y. and W.H revised and edited the manuscript. E.M.J supervised the work and critically revised the manuscript for important intellectual content. All authors have read and agreed to the published version of the manuscript.

REFERENCES

1. Westwood M, Joore M, Grutters J, et al. Contrast-enhanced ultrasound using SonoVue® (sulphur hexafluoride microbubbles) compared with contrast-enhanced computed tomography and contrast-enhanced magnetic resonance imaging for the characterisation of focal liver lesions and detection of liver metastases: a systematic review and cost-effectiveness analysis. Health Technol Assess 2013;17:1-243. doi:10.3310/hta171600
2. Strobel D, Bernatik T, Blank W, et al. Diagnostic accuracy of CEUS in the differential diagnosis of small (≤20 mm) and subcentimetric (≤10 mm) focal liver lesions in comparison with histology. Results of the DEGUM multicenter trial. Ultraschall Med 2011;32:593-597. doi:10.1055/s-0031-1271114
3. Dietrich CF, Nolsøe CP, Barr RG, et al. Guidelines and Good Clinical Practice Recommendations for Contrast Enhanced Ultrasound (CEUS) in the Liver - Update 2020 - WFUMB in Cooperation with EFSUMB, AFSUMB, AIUM, and FLAUS. Ultraschall Med 2020;41:562–585. doi:10.1055/a-1177-0530

4. Wilson SR, Feinstein SB. Introduction: 4th Guidelines and Good Clinical Practice Recommendations for Contrast Enhanced Ultrasound (CEUS) in the Liver-Update 2020 WFUMB in Cooperation with EFSUMB, AFSUMB, AIUM and FLAUS. Ultrasound Med Biol 2020;46:3483-3484. doi:10.1016/j.ultrasmedbio.2020.08.015
5. Şirli R, Sporea I, Popescu A, et al. Contrast-enhanced ultrasound for the assessment of focal nodular hyperplasia - results of a multicentre study. Med Ultrason 2021;23:140-146. doi:10.11152/mu-2912
6. Wilson SR, Burns PN, Kono Y. Contrast-Enhanced Ultrasound of Focal Liver Masses: A Success Story. Ultrasound Med Biol 2020;46:1059-1070. doi:10.1016/j.ultrasmedbio.2019.12.021
7. Franke D, Daugherty RJ, Ključevšek D, et al. Contrast-enhanced ultrasound of transplant organs - liver and kidney - in children. Pediatr Radiol 2021;51:2284-2302. doi:10.1007/s00247-020-04867-y
8. Zuo D, Yang K, Wu S. Diagnostic performance of intravascular perfusion based contrast-enhanced ultrasound LI-RADS in the evaluation of hepatocellular carcinoma. Clin Hemorheol Microcirc 2021;78:429-437. doi:10.3233/CH-211164
9. Wu XF, Bai XM, Yang W, et al. Differentiation of atypical hepatic hemangioma from liver metastases: Diagnostic performance of a novel type of color contrast enhanced ultrasound. World J Gastroenterol 2020;26:960-972. doi:10.3748/wjg.v26.i9.960
10. Wiesinger I, Jung F, Jung EM. Contrast-enhanced ultrasound (CEUS) and perfusion imaging using VueBox. Clin Hemorheol Microcirc 2021;78:29-40. doi:10.3233/CH-201040
11. Jung EM, Weber MA, Wiesinger I. Contrast-enhanced ultrasound perfusion imaging of organs. Radiologe 2021;61(Suppl 1):19-28. doi:10.1007/s00117-021-00891-7
12. Schwarz S, Clevert DA, Ingrisch M, et al. Quantitative Analysis of the Time-Intensity Curve of Contrast-Enhanced Ultrasound of the Liver: Differentiation of Benign and Malignant Liver Lesions. Diagnostics (Basel) 2021;11:1244. doi:10.3390/diagnostics11071244
13. A Pausch AM, Kammerer S, Weber F, et al. Parametric Imaging of Contrast-Enhanced Ultrasound (CEUS) for the Evaluation of Acute Gastrointestinal Graft-Versus-Host Disease. Cells, 2021;10:1092. doi:10.3390/cells10051092
14. Albrecht T, Oldenburg A, Hohmann J, et al. Imaging of liver metastases with contrast-specific low-MI real-time ultrasound and SonoVue. Eur Radiol 2003;13 Suppl 3:N79-N86. doi:10.1007/s00330-003-0012-2
15. Terzi E, Giamperoli A, Iavarone M, et al. Prognosis of Single Early-Stage Hepatocellular Carcinoma (HCC) with CEUS Inconclusive Imaging (LI-RADS LR-3 and LR-4) Is No Better than Typical HCC (LR-5). Cancers (Basel) 2022;14:336. doi:10.3390/cancers14020336
16. Chartampilas E, Rafailidis V, Georgopoulou V, Kalarakis G, Hatzidakis A, Prassopoulos P. Current Imaging Diagnosis of Hepatocellular Carcinoma," Cancers (Basel) 2022;14:3997. doi:10.3390/cancers14163997
17. Schellhaas B, Bernatik T, Bohle W, et al. Contrast-Enhanced Ultrasound Algorithms (CEUS-LIRADS/ESCULAP) for the Noninvasive Diagnosis of Hepatocellular Carcinoma - A Prospective Multicenter DEGUM Study. Ultraschall Med 2021;42:178-186. doi:10.1055/a-1220-8561
18. Strobel D, Seitz K, Blank W, et al. Contrast-enhanced ultrasound for the characterization of focal liver lesions--diagnostic accuracy in clinical practice (DEGUM multicenter trial). Ultraschall Med 2008;29:499-505. doi:10.1055/s-2008-1027806
19. Tai CJ, Huang MT, Wu CH, et al. Contrast-Enhanced Ultrasound and Computed Tomography Assessment of Hepatocellular Carcinoma after Transcatheter Arterial Chemo-Embolization: A Systematic Review. J Gastrointestin Liver Dis 2016;25:499-507. doi:10.15403/jgld.2014.1121.254.tai
20. Haimerl M, Poelsterl S, Beyer LP, et al. Chronic liver disease: Quantitative MRI vs CEUS-based microperfusion. Clin Hemorheol Microcirc 2016;64:435-446. doi:10.3233/CH-168112
21. Sansone V, Falsetti L, Tovoli F, Golfieri R, Cescon M, Piscaglia F. An Uncommon Focal iver Lesion: Intrahepatic Splenosis. J Gastrointestin Liver Dis 2020;29:257-262. doi:10.15403/jgld-617
22. Schwarze V, Rübenthaler J, Marschner C, et al. Advanced Fusion Imaging and Contrast-Enhanced Imaging (CT/MRI-CEUS) in Oncology. Cancers (Basel) 2020;12:2821. doi:10.3390/cancers12102821
23. Sporea I, Săndulescu DL, Şirli R, et al. Contrast-Enhanced Ultrasound for the Characterization of Malignant versus Benign Focal Liver Lesions in a Prospective Multicenter Experience - The SRUMB Study. J Gastrointestin Liver Dis 2019;28:191-196. doi:10.15403/jgld-180
24. Pschierer K, Grothues D, Rennert J, et al. Evaluation of the diagnostic accuracy of CEUS in children with benign and malignant liver lesions and portal vein anomalies. Clin Hemorheol Microcirc 2015;61:333-345. doi:10.3233/CH-152003
25. Chang EH, Chong WK, Kasoji SK, et al. Diagnostic accuracy of contrast-enhanced ultrasound for characterization of kidney lesions in patients with and without chronic kidney disease. BMC Nephrol 2017;18:266. doi:10.1186/s12882-017-0681-8
26. Barr RG, Huang P, Luo Y, et al. Contrast-enhanced ultrasound imaging of the liver: a review of the clinical evidence for SonoVue and Sonazoid. Abdom Radiol (NY) 2020;45:3779-3788. doi:10.1007/s00261-020-02573-9
27. Jung EM, Moran VO, Engel M, Krüger-Genge A, Stroszczynski C, Jung F. Modified contrast-enhanced ultrasonography with the new high-resolution examination technique of high frame rate contrast-enhanced ultrasound (HiFR-CEUS) for characterization of liver lesions: First results. Clin Hemorheol Microcirc 2023;83:31-46. doi:10.3233/CH-221449
28. Sosa-Valencia L, Huppertz J, Wanert F, et al. Design and validation of a therapeutic EUS training program using a live animal model: Taking training to the next level. Endosc Ultrasound 2022;11:112-121. doi:10.4103/EUS-D-21-00124
29. Giangregorio F. Contrast-Enhanced Ultrasound (CEUS) for Echographic Detection of Hepato Cellular Carcinoma in Cirrhotic Patients Previously Treated with Multiple Techniques: Comparison of Conventional US, Spiral CT and 3-Dimensional CEUS with Navigator Technique (3DNav CEUS). Cancers (Basel) 2011;3:1763-1776. doi:10.3390/cancers3021763
30. Jung EM, Dong Y, Jung F. Current aspects of multimodal ultrasound liver diagnostics using contrast-enhanced ultrasonography (CEUS), fat evaluation, fibrosis assessment, and perfusion analysis - An update. Clin Hemorheol Microcirc 2023;83:181-193. doi:10.3233/CH-239100
31. Lupușoru R, Sporea I, Rațiu I, et al. Contrast-Enhanced Ultrasonography with Arrival Time Parametric Imaging as a Non-Invasive Diagnostic Tool for Liver Cirrhosis. Diagnostics (Basel) 2022;12:3013. doi:10.3390/diagnostics12123013
32. Schaible J, Stroszczynski C, Beyer LP, Jung EM. Quantitative perfusion analysis of hepatocellular carcinoma using dynamic contrast enhanced ultrasound (CEUS) to determine tumor microvascularization. Clin Hemorheol Microcirc 2019;73:95-104. doi:10.3233/CH-199221
33. Schelker RC, Barreiros AP, Hart C, Herr W, Jung EM. Macro- and microcirculation patterns of intrahepatic blood flow changes in patients with hereditary hemorrhagic telangiectasia. World J Gastroenterol 2017;23:486-495. doi:10.3748/wjg.v23.i3.486
34. Brandenstein M, Wiesinger I, Künzel J, Hornung M, Stroszczynski C, Jung EM. Multiparametric Sonographic Imaging of Thyroid

Lesions: Chances of B-Mode, Elastography and CEUS in Relation to Preoperative Histopathology. Cancers (Basel) 2022;14:4745. doi:10.3390/cancers14194745

35. Turco S, Tiyarattanachai T, Ebrahimkheil K, et al. Interpretable Machine Learning for Characterization of Focal Liver Lesions by Contrast-Enhanced Ultrasound. IEEE Trans Ultrason Ferroelectr Freq Control 2022;69:1670-1681. doi:10.1109/TUFFC.2022.3161719.
36. Denis de Senneville B, Frulio N, Laumonier H, Salut C, Lafitte L, Trillaud H. Liver contrast-enhanced sonography: computer-assisted differentiation between focal nodular hyperplasia and inflammatory hepatocellular adenoma by reference to microbubble transport patterns. Eur Radiol 2020;30:2995-3003. doi:10.1007/s00330-019-06566-1
37. Hu HT, Wang W, Chen LD, et al. Artificial intelligence assists identifying malignant versus benign liver lesions using contrast-enhanced ultrasound. J Gastroenterol Hepatol 2021;36:2875-2883. doi:10.1111/jgh.15522
38. Dietrich CF, Averkiou M, Nielsen MB, et al. How to perform Contrast-Enhanced Ultrasound (CEUS). Ultrasound Int Open 2018;4:E2-E15. doi:10.1055/s-0043-123931